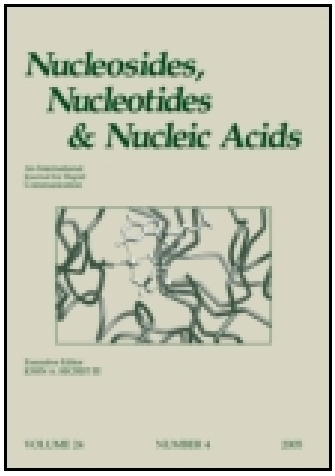

Nucleosides, Nucleotides and Nucleic Acids

Publication details, including instructions for authors and subscription information:
http://www.tandfonline.com/loi/lncn20

Synthesis, DNA-Binding, and Photocleavage Properties of a Serious of Porphyrin-Daunomycin Hybrids

Ping Zhao[a], Jia-Zheng Lu[b], Juan He[a], Wan-Hua Chen[a], Pan-Pan Chen[a], Dian-Wen Chen[a] & Qian-Yun Bin[a]

[a] School of Chemistry and Chemical Engineering, Guangdong Pharmaceutical University, NO. 13, Changmingshui Road, Zhongshan, PR China

[b] School of Pharmacy, Guangdong Pharmaceutical University, NO. 280, Waihuandong Road, Education Mega Centre, Guangzhou, PR China

Published online: 08 Aug 2014.

To cite this article: Ping Zhao, Jia-Zheng Lu, Juan He, Wan-Hua Chen, Pan-Pan Chen, Dian-Wen Chen & Qian-Yun Bin (2014) Synthesis, DNA-Binding, and Photocleavage Properties of a Serious of Porphyrin-Daunomycin Hybrids, Nucleosides, Nucleotides and Nucleic Acids, 33:9, 597-614, DOI: 10.1080/15257770.2014.912321

To link to this article: http://dx.doi.org/10.1080/15257770.2014.912321

Nucleosides, Nucleotides and Nucleic Acids, 33:597–614, 2014

ISSN: 1525-7770 print / 1532-2335 online
DOI: 10.1080/15257770.2014.912321

SYNTHESIS, DNA-BINDING, AND PHOTOCLEAVAGE PROPERTIES OF A SERIOUS OF PORPHYRIN-DAUNOMYCIN HYBRIDS

Ping Zhao,[1] Jia-Zheng Lu,[2] Juan He,[1] Wan-Hua Chen,[1] Pan-Pan Chen,[1] Dian-Wen Chen,[1] and Qian-Yun Bin[1]

[1]*School of Chemistry and Chemical Engineering, Guangdong Pharmaceutical University, Zhongshan, PR China*

[2]*School of Pharmacy, Guangdong Pharmaceutical University, Education Mega Centre, Guangzhou, PR China*

□ *It is widely accepted that the pharmacological activities of anthracyclines antitumor agents express when the quinone-containing chromophore intercalates into base pairs of the duplex DNA. We have successfully synthesized and investigated the DNA-interactions of hybrids composed with quinone chromophore and cationic porphyrin. Herein, a clinic anticancer drug, daunomycin, is introduced to the porphyrin hybrids through different lengths of amide alkyl linkages, and their interactions and cleavage to DNA were studied compared with the previous porphyrin-quinone hybrids. Spectral results and the determined binding affinity constants (K_b) show that the attachment of daunomycin to porphyrin could improve the DNA-binding and photocleaving abilities. The porphyrin-daunomycin hybrids may find useful employment in investigating the ligand-DNA interaction.*

Keywords Porphyrin-daunomycin hybrids; DNA binding; DNA photocleavage

INTRODUCTION

Anthracyclines represent an important class of antitumor agents. Daunomycin (DNR), which is the lead compound in the series, is routinely used in the clinic for the treatment of leukemia, as well as for ovarian and breast carcinoma.[1, 2] Although DNR is highly efficient antineoplastic agent, its clinical use is limited due to clinical and histopathologic evidence of cardiotoxicity.[3–5] In the past years, numerous anthracyclines derivatives have been synthesized with the aim of finding related compounds showing better therapeutic efficacy together with fewer side effects.[6–8] Biochemical evidence suggests that, in common with the anthracycline anticancer drugs,

Received 24 July 2013; accepted 2 April 2014.

Address correspondence to Dr. Ping Zhao, School of Chemistry and Chemical Engineering, Guangdong Pharmaceutical University, No. 13, Changmingshui Road, Zhongshan 528458, PR China. E-mail: zhaoping666@163.com

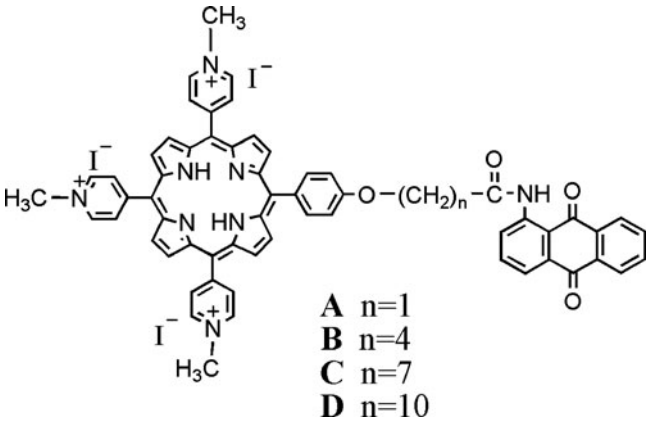

FIGURE 1 The structures of Por-AQ hybrids.

DNA is among the principal cell targets of these drugs and the pharmacological activities of DNR express when the quinone-containing chromophore intercalates into base pairs of the duplex DNA. The intercalative efficiency of drugs to DNA will remarkably influence the pharmacological activity. The chemical modifications of DNR, which have commonly been considered, concern either the nature or position of the aminoacyl side chains or the chromophore unit.[9–11] The hope of finding noncardiotoxic yet active anthracycline antitumor antibiotics has spurred the search for new occurring anthracycline and research in synthesizing new DNR analogues.

Porphyrins' unique character of high accumulation in the cancer cells gives us the inspiration of designing new porphyrin- DNR hybrid to facilitate the accumulation of drugs in cancer cells and thus decrease the cardiotoxicity of the anthracycline. Specially, cationic porphyrins (Por) are preferentially considered for its additional tight intercalation into DNA and thus are expected to enhance the DNA binding abilities of the drugs additionally. We have previously linked cationic porphyrin and anthraquinone (AQ), which is the core chromophore unit of DNR, with various lengths of flexible alkyl links (see structures in Figure 1), and found that these cationic water-soluble Por-AQ derivatives bind with DNA and give rise to DNA photocleavage.[12,13] So far no porphyrin-DNR hybrids have been reported. It remains uncertainty that whether the biological activities will be different when clinic DNR structure linked with porphyrin and whether the porphyrins could actually increase the DNA binding and cleavage ability of DNR.

Our promising results encourage us to research further in this field. In the present work, we attached the clinic DNR molecules to cationic porphyrin through different flexible carbochains and tested their DNA binding and photocleavage abilities. Since the DNR structure has additional sugar groups and positive charge compared with the single AQ chromophore unit,

it is expected that the modified Por-DNR hybrids will be more favorable in biological activities and bring us new surprise.

RESULTS AND DISCUSSION

Synthesis

We have successfully obtained Por-AQ hybrids by attaching flexible carbochains to the anthraquinone molecules firstly and then linked to the porphyrin moiety.[13] However, this experience failed in synthesizing Por-DNR hybrids because the DNR molecule has more active groups than AQ. Without the complex and troublesome group protection process, the active OH and NH_2 groups in DNR molecules will form rings when react with brominated carbon chains. However, many reports on the synthesis of DNR derivatives have concluded that the NH_2 group has much higher nucleophilicity than OH groups and thus without group protection, nucleophilic reactions could selectively occur on the NH_2 group rather than on the OH groups of the DNR molecules at room temperature.[16–18] Encouraged by these reports, we firstly chemically modified the porphyrin part with dibromo alkanes and porphyrin derivatives with an active Br at the end of the flexible carbon chains were obtained. Then, this active Br could selectively react with the NH_2 group in DNR molecules at room temperature and Por-AQ hybrids were successfully synthesized (see Scheme 1). In this synthetic process, no group protection reactions were needed. This method has the advantages of high productivity and effortlessness.

DNA-binding Properties

Absorption Titrations

The hybrids exhibit intense absorption band around 430 nm and weaker bands from 500–600 nm, which are attributed to porphyrin ring, namely Soret band and Q bands, respectively. Meanwhile, DNR's characteristic absorption, centered at 290 nm and 475 nm were also clearly observed. With the increasing of DNA concentration, the absorption spectra of the cationic Por-DNR hybrid **3** at both the porphyrin and DNR's characteristic absorption range are remarkably disturbed with large hypochromism and bathochromism. This is an intuitional evidence of the drug-DNA binding behavior. We gave the absorption spectral changes upon DNA addition of compounds **1, 2** and **3** as Figure S3 in supplemental materials.

Table 1 summarizes the detailed titration data on DNA of all these three Por-DNR compounds. From table 1, the porphyrin moieties for the Por-DNR compounds **2** and **3** have comparable hypochromism and red shift at around 430 nm with those of Por-AQ compounds **B**, **C**, and **D**, suggesting

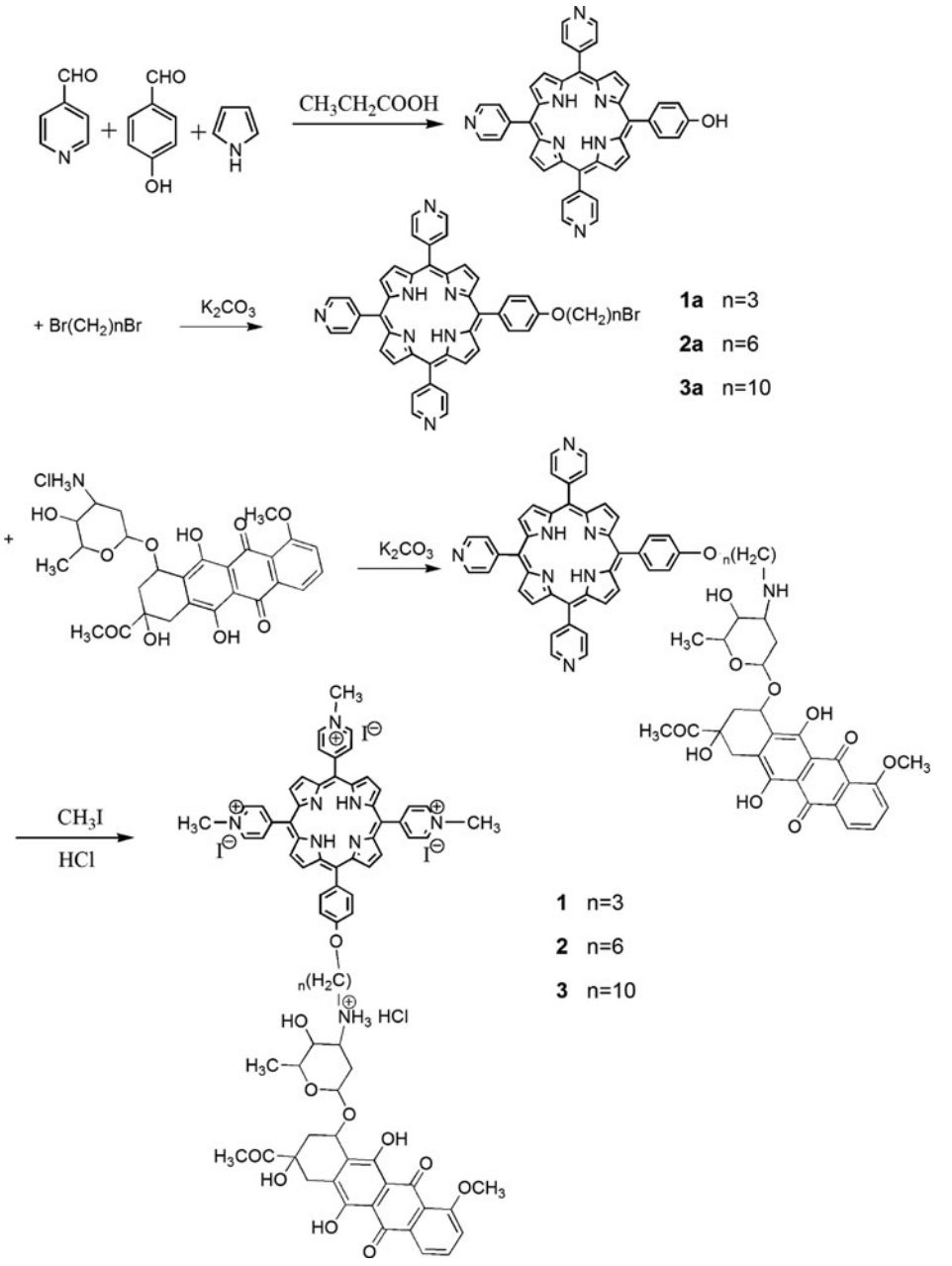

SCHEME 1 The synthetic scheme of cationic Por-DNR hybrids.

that the porphyrin parts in these two kinds of hybrids may have similar DNA-binding behaviors.[13] Meanwhile, compound **1** exhibit similar DNA-binding property with compound **A**. [12] However, the absorption spectral ranges centered at 290 and 475 nm attributed to DNR for compounds **2**

TABLE 1 Physical data of Por-DNR hybrids binding with CT DNA

Compound	UV-Vis spectra		ICD spectra		ΔT_m	K_b Por DNR	Por-DNR
	$\Delta\lambda$(nm)	H%	$\Delta\lambda$(nm)	H%	°C	$\times 10^6$ M^{-1}	
1	7	34.52	10	42.11	+ -	7.9	5.8
2	13	46.31	9	47.52	+ -	+ 11.1	8.2
3	16	51.38	11	52.88	+ -	+ 13.2	9.3

and **3** have much larger hypochromism compared with those of AQ part for corresponding Por-AQ hybrids. Since large degree of hypochromism is an important signal for intense DNA-binding, we suppose the DNR moieties in the studied hybrids have higher interactions than AQ moieties we reported before. The sugar chain in DNR seems play a significant role in the DNA-binding behavior, whereas a conclusion as to the specific binding mode of these Por–DNR dyads cannot be made from this method alone.

Fluorescence Studies

Fluorescence Titration Studies

Fluorescence titration experiments of the compounds in the presence of CT DNA were performed. When excited with 420 nm (porphyrin's excitation wavelength) or 475 nm (DNR's excitation wavelength), the hybrids have similar emission spectra, ranging from 520 to 670 nm. Fluorescence emission spectra of these compounds with increasing DNA were given as Figure S4 in the supplemental materials, from which we can find that the fluorescence intensities of these cationic Por-DNR hybrids are remarkably enhanced with the increase of DNA. Since the hydrophobic environment provided by DNA can protect the compound from quenching by water molecules, the emission increase is widely admitted as an indication of the interaction between drugs and DNA.[19, 20] Thus, the large emission increase suggests that the hybrids interact with DNA rather strongly.

Fluorescence Emission Quenching Studies

For drugs with positive charges, Steady-state emission quenching experiment was often employed to evaluate the DNA binding of positively charged compounds. Figure 2 gives **1** as an example to illustrate the quenching effect of $K_4Fe(CN)_6$ on the fluorescence intensities of compound in the absence and presence of CT DNA. From Figure 2, we can find that in the absence of CT DNA, the weak fluorescence of **1** is completely quenched at the initial stage of ($K_4Fe(CN)_6$) addition. However, in the DNA–drug system, there is no substantial change on the fluorescence intensity of **1** with increasing ($K_4Fe(CN)_6$) concentrations. This may be explained by the fact that the bond cations of the compounds are protected from the anionic water-bound

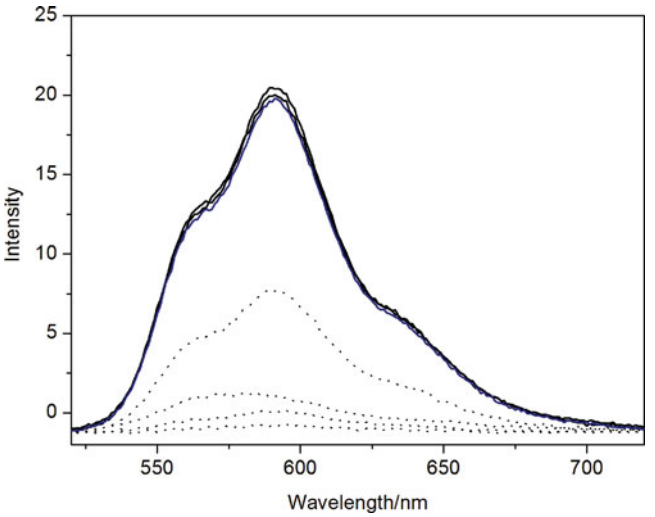

FIGURE 2 Emission quenching curves with $K_4Fe(CN)_6$ for free (dot line) and DNA-bound (solid line) **1** in buffer A. [Drug]/[DNA] = 0.25 (Color figure available online).

quencher by the array of negative charges along the DNA phosphate backbone.[21] Similar results were obtained in the case of **2** and **3**, suggesting that all these compounds can bind to the DNA rather strongly.

Competitive Binding Experiments with EB

In order to compare quantitatively, their binding affinity constants (K_b) to CT DNA have to be measured. For compounds with multiple binding sites, traditional UV–Vis titration method is not suitable to determine K_b between compounds and DNA.[12, 22] Fluorescence spectrum was used to measure K_b by competition between EB and the studied compounds for binding to DNA. This method measures the decrease of fluorescence of EB bound to DNA in the presence of the compound of interest. It can be used for all compounds having a good affinity for DNA whatever their binding modes may be because it only measures the ability of a compound to prevent intercalation of EB into DNA. [12, 19, 22]

The EB competitive binding experiments were carried out and quenching plots are given in Figure S5 of supplemental materials. The quenching plots of I_0/I *vs* [Drug]/[DNA] are in good agreement with the linear Stern-Volmer equation with slopes of 3.63, 5.16, and 5.78 for **1**, **2**, and **3**, respectively. We can also learn from Figure S5 that 50% of EB molecules were replaced from DNA-bound EB at a concentration ratio of [Drug]/[EB] = 1.72, 1.21, and 1.08 for **1**, **2**, and **3**, respectively. By taking K_b of 1.0×10^7 M^{-1} for EB under this experimental condition [22], the K_b of **1**, **2**, and **3** were derived 5.8×10^6 M^{-1}, 8.2×10^6 M^{-1}, and 9.3×10^6 M^{-1} (K_b(EB)/1.72,

K_b(EB)/1.21, and K_b(EB)/1.08), respectively.[23] The DNA binding affinities of the Por-DNR hybrids with longer bridging links (**2** and **3**) are higher than that with shorter bridging link (**1**). This can be explained by the fact that both two moieties in the long-linked hybrids intercalate into DNA and both can replace EB from DNA helix, leading to relatively high binding affinities. Meanwhile, the K_b of these Por-DNR hybrids are a little larger than those of Por-AQ hybrids [12, 13], indicating that the additional positive charge and the appending sugar chain are beneficial for the binding affinities of hybrids.

ICD Spectra

The ICD spectrum experiment is widely accepted as one of the most direct means in examining the binding modes of the small molecules to DNA. [12, 13, 19–24] None of these compounds as well as DNA by themselves displays any CD spectra signal in the visible region, but ICD spectra are observed in these compounds with DNA titration. It is well known that a positive ICD peak is due to groove binding and a negative ICD peak is due to intercalative binding.[12,19]

Figure 3 illustrates the ICD spectra and Table 1 lists the ICD spectral signals for these Por-DNR compounds bound to CT DNA. The observed ellipticities ranging from 360 to 430 nm could be attributed to the Por moiety while those from 450 to 500 nm are for DNR moiety. From Figure 3, for hybrids **1** and **2**, the ICD signal at porphyrin's range show both positive and negative peaks which become stronger with the titration of DNA. This result indicates that the Por moieties in these two compounds employ both intercalation and groove binding when bound to DNA. However, in the presence of DNA, hybrid **3** exhibit predominantly negative signal. With the addition of DNA, the negative signal of ICD spectra becomes stronger. Since the negative ICD signal is diagnostic of intercalative binding, this result confirms that the Por moiety of **3** mainly intercalate into the DNA duplex under the experimental conditions. As to the DNR part, for hybrids **2** and **3**, strong positive ICD peaks were observed, indicating the intensive DNA groove binding of DNR in these two compounds. Combining with the large hypochromism and bathochromism in DNR's absorption of hybrids **2** and **3**, the ICD signals support the reported conclusion that DNR moiety is not just simply lying in the minor groove with the functional group of sugar interact with the base pairs of DNA, and the anthraquinone plane also intercalates into the DNA double helix structure. [25–27]

One the other hand, no substantial ICD signal was found for hybrid **1** in DNR's range, suggesting that the interaction between DNR moiety of **1** with DNA is relatively weak, which possibly through electrostatic attraction between the positive charge of the DNR moiety and the negative DNA phosphate backbones. It is likely that, because of the short linkage in

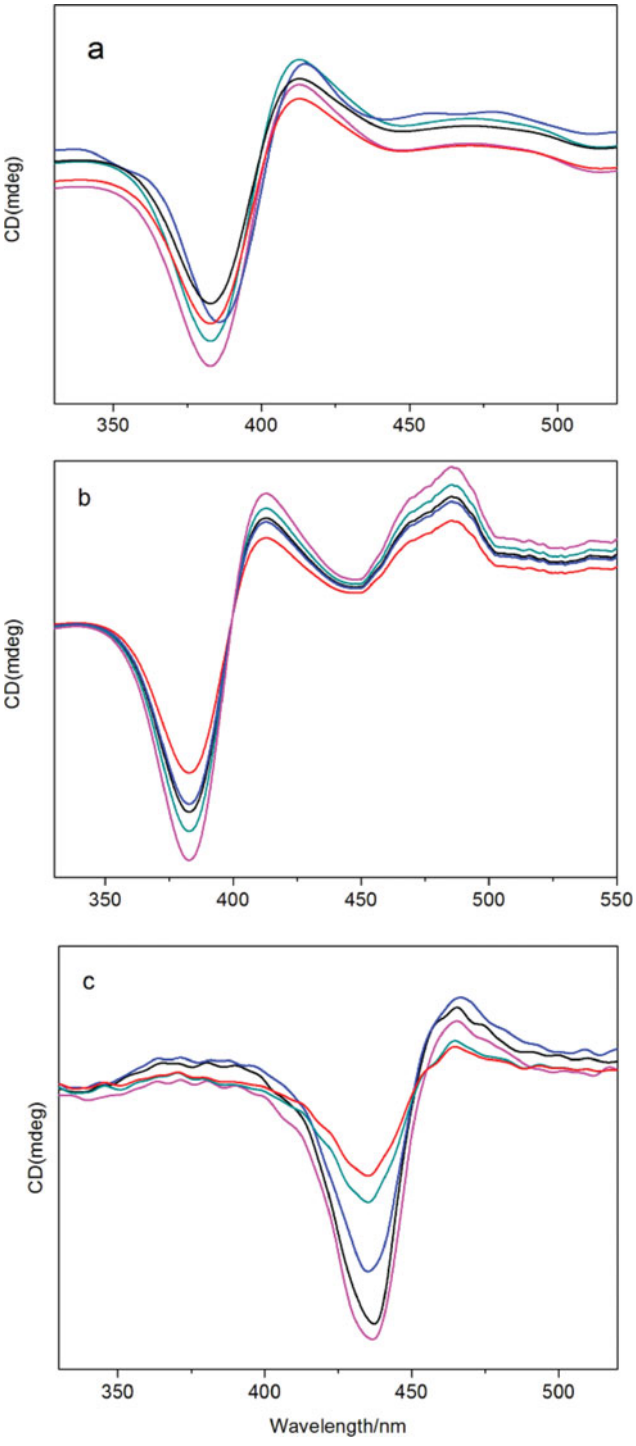

FIGURE 3 ICD spectra of Por-DNR hybrids **1** (a), **2** (b), and **3** (c) in the presence of CT DNA in buffer A. [Drug] = 10 μM, [Drug]/[DNA] = 0.3(—), 0.2(—), 0.15(—), 0.10(—), and 0.05.(—) (Color figure available online).

hybrid **1**, there is steric hindrance between the porphyrin and DNR moieties and it is difficult for both the two moieties intercalate in DNA base pairs. This conclusion is similar to that we got from the DNA binding of Por-AQ hybrids and the effect of linkage lengths seems still exist in spite of higher positive charge and sugar groups. [12,13] The distinct ICD signals of these compounds are in good consistent with foregoing experimental results.

Thermal Denaturation Studies

The thermal denaturation of double-helical polynucleotides from double stranded to single stranded is manifested as hyperchromism in the UV absorption. The melting temperature (T_m) of DNA is sensitive to its double-helix stability and the binding of compounds to DNA alters the T_m value, with dependence on the strength of the interactions. [25] Upon binding of small molecules to DNA, the T_m value of the B-form DNA should become higher, as compared to that of unbound or free DNA. In addition, as the small molecules bind more strongly to the DNA, the increase in the T_m value will become larger. Therefore, the T_m value can be used as an indicator of the binding properties and binding strengths of compounds with DNA. [19, 28]

The melting curves of CT DNA in the absence and presence of compounds are presented in Figure 4. Under the present experimental conditions, the melting curve has a transition, and the T_m value of free double-stranded CT DNA is $(60.4 \pm 0.2)^\circ$C; when mixed with the compounds, the observed melting temperatures of CT DNA increase to different extents and the increases of T_m (ΔT_m) are summarized in Table 1.

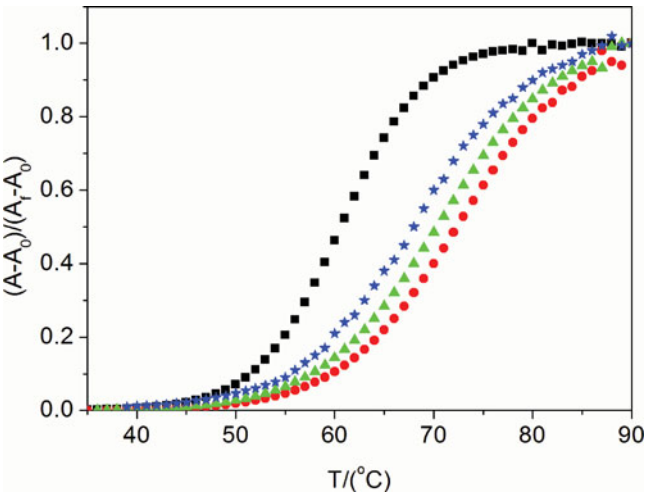

FIGURE 4 Melting curves of CT DNA at 260 nm in the absence (■) and presence of **1** (☆), **2** (▲), and **3** (●), in buffer B. [Drug] = 10 μM, [DNA] = 100 μM (Color figure available online).

From Table 1, we can find that the values of ΔT_m in the presence of **1**, **2,** and **3** are relatively large, suggesting that the compounds have strong DNA binding affinities. The much larger increases of **2** and **3** than **1** could be understood by the intense interact of both Por and DNR moieties of these two hybrids. It is reasonable if one concludes from this result that **1** mainly binds with DNA through its cationic Por moiety while the DNR moiety may only bind with DNA through its sugar chains and positive charge rather than the intercalate with anthraquinone chromophore. This result is in consistent with the ICD spectra from which we could observe negligible DNR signal of **1**. However, for hybrids **2** and **3** with longer links, besides the tight DNA interaction of their Por moieties, the higher ΔT_m indicates that their DNR moieties also intercalate into DNA duplex, too. Thus, the results of thermal denaturation further argue for the DNA binding modes we mentioned above.

Viscosity Analysis and Equilibrium Dialysis

Without X-ray structural data Hydrodynamic methods which are sensitive to changes in the length of DNA are arguably the most critical test of the classical intercalation model, and therefore they provide the most definitive means of inferring the binding mode of DNA in solution. [19] Intercalation mode is expected to lengthen the DNA helix as the base pairs are pushed apart to accommodate the bound ligand, leading to an increase in the DNA viscosity. In contrast, a partial, nonclassical intercalation of ligand could bend (or kink) the DNA helix and reduce its effective length and, concomitantly, its viscosity. When outside binding or groove binding occurs, the viscosity of DNA will not change basically. [29, 30] The viscosity of the buffer solutions of CT DNA increases with the addition of the compounds, **1**, **2**, and **3** (Figure 5). Such an increase provides striking evidence for the intercalation of these hybrids into the DNA duplex. As expected, hybrids **2** and **3** show relatively higher viscosity than that of hybrid **1**.

Red precipitations were observed visually when we attempted to research the DNA viscosity change at higher drug concentrations, similar to what happened in the Por-AQ hybrids study. This phenomenon is common in the viscosity research of cationic drugs with DNA and can be ascribed to the external binding mode between the positive macrocycles and the negative phosphate backbone. [31, 32] Equilibrium dialysis experiments were thus also carried out to investigate the DNA binding behaviors of these compounds at a [Drug]/[DNA] ratio of 0.08 and the results are summarized in Figure 6 as a histogram. As is shown in Figure 6, under identical experimental conditions, the amounts of the hybrids bound to CT DNA decreased in the order of **3** > **2** > **1**. This order is in good agreement with the results of spectra and thermal denaturation studies above and should be closely correlated with their DNA-binding affinities.[33]

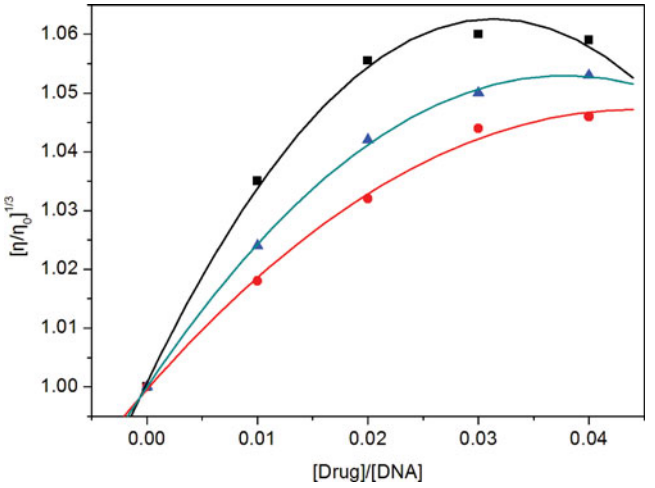

FIGURE 5 Plots of the relative viscosity change of CT DNA in the presence of **1** (●), **2** (▲), and **3** (■) in buffer A at (30 ± 0.1)°C. [DNA] = 0.5 mM (Color figure available online).

DNA Photocleavage

We compared the DNA photocleavage abilities of Por-DNR and Por-AQ hybrids under identical irradiation by high pressure lamp, whose main emission wavelengths centered at 253.65, 435, and 546 nm, and gave the results in Figure 7. Without irradiation, no substantial cleavage of DNA was observed for all the hybrids (data not shown). Under irradiation, these Por-DNR hybrids show higher DNA photocleavage activities than Por-AQ hybrids.

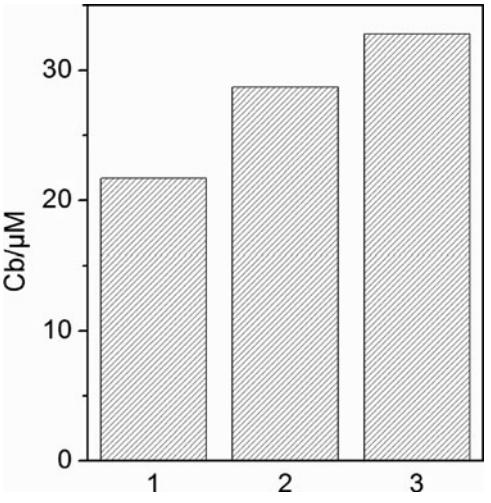

FIGURE 6 The amounts of Por-DNR hybrids bound to CT DNA (C_b) in dialysate buffer (10 mM sodium phosphate, pH 7.0). [DNA] = 0.5 mM, C_t = 50 μM, dialyse for 24 hours at 25°C.

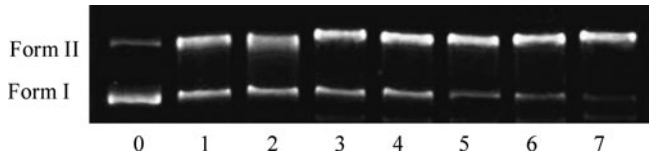

FIGURE 7 Photocleavage of pBR322 plasmid DNA after irradiated by high pressure mercury lamp (b). Ten microliters reaction mixtures contained 1.0 μg of plasmid DNA in buffer C. [Drug] = 2 μM. Lane 0: untreated DNA, no irradiation; Lanes 1∼7: in the presence of **A, B, C, D, 1, 2,** and **3,** respectively, irradiation for 20 minutes.

We have investigated the DNA photocleavage abilities of a serious cationic porphyrins with different positive charges and conclude that more positive charges and smaller steric hindrance of porphyrin will lead to a higher DNA photocleavage efficiency.[14] This expected result here further proved the conclusion above and the Por-DNR hybrids were considered better potential DNA photocleaving agents. These results are in high consistent with previous reports on the relationship between DNA binding and photocleavage of cationic porphyrins. [14, 34, 35]

We investigated the influence of different potentially inhibiting agents on the DNA photocleavage of the Por-DNR hybrids with longer links. Figure 8 shows the DNA photocleavage by **1** in the presence of inhibiting agents under irradiation with visible light. The percentage of Form II DNA after photoirradiation in the presence of **1** was decreased by the addition of NaN_3, which is known to be a scavenger of $^1O_2$.[35] When the sample solutions were thoroughly degassed with nitrogen gas and maintained under N_2 during the experiment, the DNA photocleavage was greatly inhibited as compared with that in air. In addition, the photocleavage ability was substantially enhanced by replacing the reaction media H_2O by 70% D_2O which makes the life span of $^1O_2$ longer. These results suggest that the pathway to produce Form II DNA is aerobic and $^1O_2$ are the reactive species responsible for the DNA photocleavage. On the other hand, hydroxyl radical is hardly involved in the DNA photocleavage by **1** since the addition of ethanol, methanol and DMSO, which are known as scavengers of hydroxyl radical, did not significantly affect the percentage of Form II DNA. Similar cases were observed for **2** and **3**.

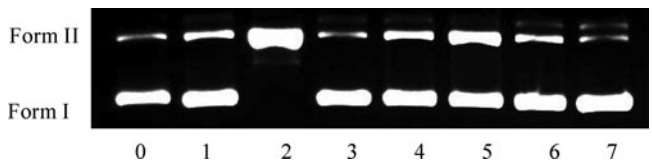

FIGURE 8 Photocleavage of pBR322 plasmid DNA in the presence of **1** and different inhibitors after irradiation by high pressure mercury lamp for 15 minutes. Ten microliters reaction mixtures contained 1.0 μg of plasmid DNA in buffer C. [Drug] = 1.5 μM. Lane 0: DNA control; lane 1: in the presence of 1, no inhibitor; lanes 2–6: in the presence of 1 and inhibitor: (2) 70% D_2O, (3) NaN_3 (5 mM), (4) DMSO (5 mM), (5) ethanol (5 mM), (6) methanol (5 mM), and (7) under an Ar atmosphere.

TABLE 2 The slopes of the plots of the consumption of DMFU by photosensition of hybrids

	1	**2**	**3**	**A**	**B**	**C**	**D**
S^a	2.8	2.4	2.6	1.3	1.9	1.5	1.8

a. *S* refers to the consumption of DMFU versus illumination time. $[S] = \times 10^{-4}$mol.min^{-1}.

Photosensitized productivity of $^1O_2$ was estimated quantitatively by measuring the concentration consumption of DMFU.[36] The slopes of the plots of the consumption of DMFU versus illumination time are listed in Table 2. The specific changes were given in supplemental materials (Figure S6). We could find from table 2 that the Por-DNR hybrids have higher $^1O_2$ yields than those Por-AQ hybrids. It was widely accepted that, the long-linked cationic porphyrin-drug hybrids are much easily to form intermolecular dimmer through self-aggregation in aqueous buffer. The dimmers are inactive in yielding $^1O_2$ since the generated $^1O_2$ could be easily quenched by the aggregated molecules.[37–39] The positive charges on DNR parts of Por-DNR hybrids will relax the intermolecular self-aggregation because of the electrostatic repulsion. Thus, the Por-DNR hybrids have higher $^1O_2$ yields which finally result in higher DNA photocleavage efficiencies.

The experimental protocol used here is useful in the preliminary evaluation of the mechanism of DNA photocleavage, although it lacks the accuracy to elucidate the mechanism of DNA photocleavage in some respects.[34] Therefore, these conclusions will have to be checked by a more precise protocol with the use of end-labeled oligodeoxynucleotides in the future.[40]

CONCLUSION

Here, the authors introduced a series of cationic Por-DNR hybrids with various bridging links and investigated their binding behaviors with CT DNA as well as photocleavage activities to plasmid DNA. Spectral, thermodynamic and hydrodynamic experiments indicate the Por and DNR units in hybrids **2** and **3** with longer linkages are sterically appropriate to bis-intercalation through their porphyrin and anthraquione plane while those of **1** suffer from severe steric strains in binding with DNA. Moreover, the Por-DNR hybrids have higher DNA binding and photocleavage abilities than Por-AQ hybrids which we reported previously. The additional positive charge and sugar chain in DNR seems very beneficial in drug-DNA interactions. The porphyrin-daunomycin hybrids may find useful employment in investigating the ligand-DNA interaction. Further efforts on the biological research such as cytotoxicity and cellular uptake are currently underway.

EXPERIMENTAL

Materials and Chemicals

Por-AQ hybrids **A**, **B**, **C,** and **D** were synthesized by the methods we reported before.[13] 5-(4-Hydroxyphenyl)-10,15,20-tris(4-Npyridiniumyl) porphyrin (HTPyP) was previously synthesized.[14] Daunorubicin hydrochloride (Sigma), 1,3-dibromopropane, hexamethylene dibromide and 1,9-dibromononane (Sigma), silica gel (Qingdao), and chloroform (Guangzhou) were commercially available and of analytical grade. CT DNA and pBR322 supercoiled plasmid DNA were obtained from the Shanghai Sangon Biotech Co., Ltd. Buffer A (5 mM Tris-HCl, 50 mM NaCl, pH = 7.2, Tris = Tris(hydroxymethyl)aminomethane) solution was used in spectral, viscosity and EB competing experiments and buffer B (1.5 mM Na_2HPO_4, 0.5 mM NaH_2PO_4, 0.25 mM Na_2H_2EDTA, pH = 7.0, H_4EDTA = N,N′-ethane-1,2-diylbis[N-(carboxymethyl)glycine]) was employed for thermal denaturation studies. Gel electrophoresis studies were carried out in buffer C (50 mM Tris-HCl, 18 mM NaCl, pH = 7.2). A solution of CT DNA in buffer A gave a ratio of UV absorbance at 260 and 280 nm of 1.85:1, indicating that the CT DNA was sufficiently free of protein. The CT DNA concentration per nucleotide was determined by absorption spectroscopy using the molar absorption coefficient (6600 M^{-1} cm^{-1}) at 260 nm.[15]

Element analysis (C, H, and N) was carried out with a Perkin-Elmer 240 Q elemental analyzer. ^1H NMR spectra were recorded on a Varian-300 spectrometer. All chemical shifts are given relative to tetramethylsilane (TMS). Electrospray Ionization mass spectra (ESI–MS) were recorded on a LCQ DECA XP system (Thremo, USA). UV–Vis spectra were recorded on a Perkin-Elmer-Lambda-850 spectrophotometer. Emission spectra were recorded on a Perkin-Elmer L55 spectrofluorophotometer. CD spectra were recorded on a JASCO-J810 spectrometer. Viscosity measurements were carried out with an Ubbelohde viscometer maintained at a constant temperature of $(30 \pm 0.1)^\circ C$ in a thermostatic bath. Flow time was measured with a digital stopwatch.

For the gel electrophoresis experiment, supercoiled pBR322 DNA was treated with the compounds in the buffer (50 mM Tris–HCl, 18 mM NaCl, pH 7.2), and the solution was then irradiated at room temperature with a high presser mercury lamp. The samples were analyzed by electrophoresis for 1.5 h at 80 V on a 1% agarose gel in Tris–HCl buffer. The gel was stained with 1 lg/mL ethidium bromide and photographed on an Alpha Innotech IS–5500 fluorescence chemiluminescence and visible imaging system.

The yields of singlet oxygen were estimated by the reaction between singlet oxygen and 2,5-diamethylfuran (DMFU). The reaction was carried out in methanol solution which contains a hybrid (100 μM), DMFU (0.1M), and pyridine (0.6 M). The reaction solution was illuminated by the mercury lamp-light with a yellow light filter to get visible light ($\lambda > 470$ nm). The

concentration of DMFU was monitored by Gas Chromatography (GC-7890II) using nonane as an internal standard.

Synthesis and Characterization

Synthesis of Porphyrin Derivates

5-(1-bromopropylhydroxylphenyl)-10,15,20-tris(4-pyridiniumyl)-porphyrin (BrPPTPyP) 5-(4-hydroxyphenyl)-10,15,20-tris(4-*N*-pyridiniumyl) porphyrin (HTPyP) was dissolved in a mixture of N,N-dimethylformamide (DMF) 6 mL. Then, Na_2CO_3 (100 mg) and hexamethylene dibromide (68.7 mg, 0.26 mmol) were added. The reaction mixture was stirred at room temperature for 20–28 hours. The progress of the reaction was monitored by TLC. After the reaction was complete, the reaction mixture was diluted with $CHCl_3$ and poured into water. The organic layer was separated and washed with water until neutral pH, dried over anhydrous Na_2SO_4, and evaporated under diminished pressure. The crude product was purified by column chromatography. The final product was isolated as the objective BrHPTPyP to give a red solid (178 mg, 0.153 mmol) in 61.5% yield. ESI-MS *m/z* 753.2 ($[M\text{-}H]^-$, calcd for $C_{44}H_{32}BrN_7O$: 754.3).

5-(bromohexylhydroxylphenyl)-10,15,20-tris(4-pyridiniumyl)-porphyrin (BrHPTPyP) and *5-(1-bromodecylhydroxylphenyl)-10,15,20-tris(4-pyridiniumyl)-porphyrin (BrDPTPyP)* were similarly prepared, replacing 1,3-dibromopropane by hexamethylene dibromide and 1,10-dibromononane, respectively.

BrHPTPyP. Yield: 63.2%. ESI-MS *m/z* 795.2 ($[M\text{-}H]^-$, calcd for $C_{22}H_{22}BrNO_3$: 796.2).

BrDPTPyP. Yield: 68.6%. ESI-MS *m/z* 851.3 ($[M\text{-}H]^-$, calcd for $C_{22}H_{22}BrNO_3$: 852.3).

Synthesis of Por-DNR Hybrids

The synthetic scheme of Por-DNR hybrids is shown in Scheme 1.

Synthesis of compound **1**. Daunorubicin hydrochloride was firstly dissolved in double distilled water and 5% NaOH solution was added to adjust the pH to 10. The daunorubicin was then precipitated and extracted by dichloromethane. The organic phrase was evaporated and the deprotonated daunorubicin was obtained after drying under vacuum. Deprotonated daunorubicin (0.5 mmol, 0.272 g) and anhydrous K_2CO_3 (0.7 g) in dry DMF (20 mL) were stirred for 2 hours at room temperature. Then BrPPTPyP (0.5 mmol, 0.376 g) was added to the activated daunorubicin, and the mixture was then stirred for 36 hours at room temperature. The progress of the reaction was monitored by TLC. The reaction mixture was then diluted by $CHCl_3$ and DMF was washed out by water. The extracted crude material was purified by chromatography. Evaporation of solvent afforded compound **1a** as a purple powder (yield: 0.394 g, 65%). **1a** was methylated in 5 mL of DMF with methyl iodide (0.8 ml) for 3 hours at room temperature. The solvent and

methyl iodide were removed under vacuum. Subsequently, the residue was dissolved in a 1 M solution of hydrochloride in methanol and then precipitated with ethyl ether as hydrochloride salt, which was washed with ethyl ether until neutral pH and dried under vacuum. Compound **1** was thus obtained quantitatively. Yield: 0.384 g, 94%. (Found: C, 67.38; H, 6.13; N, 8.32%. Calc. for $C_{75}H_{73}I_3O_{11}N_8.4H_2O$: C, 67.51; H, 6.07; N, 8.40%). ESI-MS *m/z* 319.3 (M^{4+}, calcd for $C_{75}H_{73}O_{11}N_8$: 1262.4). ^{1}H NMR (300 MHz, DMSO): chemical shift δ 13.9 (s, 2H, cyclo-OH), 9.37(d, $J = 5.9$ Hz, 6H, 2, 6-pyridinium), 9.26(s, 4H, β-pyrrole), 9.03(d, $J = 6.6$ Hz, 4H, β-pyrrole), 8.90(s, 6H, 3,5-pyridinium), 8.65(s, 2H, 2, 6-phenyl), 8.01(s, 2H, 3,5-phenyl), 7.08(s, 2H, phenyl-OH), 5.49 (d, 8H, $J = 3.4$ Hz, cyclo-H), 5.09(s, 1H, NH), 4.73(s, 9H, N^+-Me), 4.68 (s, 2H, OH), 4.07 (s, 3H, OMe), 3.64 (s, 3H, DNR-phenyl), 2.4 (s, 6H, CH_3), 1.18–1.90(m, 12H, -$(CH_2)_3$-), and -3.10(s, 2H, NH pyrrole).

Compounds **2** and **3** were similarly prepared, replacing BrPPTPyP by BrHPTPyP and BrDPTPyP, respectively.

2, yield: 89%. (Found: C, 69.13; H, 6.22; N, 8.23%. Calc. for $C_{78}H_{78}I_3O_4N_8.3H_2O$: C, 69.03; H, 6.19; N, 8.26%). ESI-MS *m/z* 330.3 (M^{4+}, calcd for $C_{78}H_{78}O_4N_8$:1304.2). ^{1}H NMR (300 MHz, DMSO): chemical shift δ: 13.6 (s, 2H, cyclo-OH), 9.32(d, $J = 5.9$ Hz, 6H, 2, 6-pyridinium), 9.21(s, 4H, β-pyrrole), 9.03(d, $J = 6.6$ Hz, 4H, β-pyrrole), 8.90(s, 6H, 3,5-pyridinium), 8.63(s, 2H, 2, 6-phenyl), 8.01(s, 2H, 3,5-phenyl), 7.02(s, 2H, phenyl-OH), 5.49 (d, 8H, $J = 3.4$ Hz, cyclo-H), 5.09(s, 1H, NH), 4.73(s, 9H, N^+-Me), 4.68 (s, 2H, OH), 4.07 (s, 3H, -OMe), 3.64 (s, 3H, DNR-phenyl), 2.4 (s, 6H, CH_3), 1.18–1.90(m, 12H, -$(CH_2)_6$-), and -3.13(s, 2H, NH pyrrole).

3, yield: 87% (Found: C, 68.44; H, 6.65; N, 7.78%. Calc. for $C_{82}H_{86}I_3O_{11}N_8.4.5H_2O$: C, 68.38; H, 6.61; N, 7.78%). ESI-MS *m/z* 344.1 (M^{4+}, calcd for $C_{82}H_{86}O_{11}N_8$:1360.3).^{1}H NMR (300 MHz, DMSO): chemical shift δ: 13.4 (s, 2H, phenyl-OH), 9.31(d, J = 5.9 Hz, 6H, 2, 6-pyridinium), 9.22(s, 4H, β-pyrrole), 9.03(d, $J = 6.6$ Hz, 4H, β-pyrrole), 8.90(s, 6H, 3,5-pyridinium), 8.63(s, 2H, 2, 6-phenyl), 8.01(s, 2H, 3,5-phenyl), 7.01(s, 2H, cyclo-OH), 5.44 (d, 8H, $J = 3.4$ Hz, cyclo-H), 5.09(s, 1H, NH), 4.73(s, 9H, N^+-Me), 4.65 (s, 2H, OH), 4.07 (s, 3H, -OMe), 3.64 (s, 3H, DNR-phenyl), 2.4 (s, 6H, CH_3), 1.18–1.90(m, 20H, -$(CH_2)_{10}$-), and -2.92(s, 2H, NH pyrrole).

All the data of NMR (Figure S1) and MS (Figure S2) was provided as supplementary materials.

SUPPLEMENTAL DATA

Supplementary data for this article can be accessed at [publisher's weblink].

REFERENCES

1. Blanka, R. Clinical experience with anthracycline antibiotics–HPMA copolymer–human immunoglobulin conjugates. *Adv. Drug Deliver. Rev.* **2009**, 61, 1149–1158.

2. Pandelis, S.; Marios, P.; Carsten, W.L.; Lucas, K.; Andriani, K.; Soteroulla, C.; Elena, K.; Emanuel, K.; Nicholas, P.A.; George, S.; Marina, K. Compounds of the anthracycline family of antibiotics elevate human γ-globin expression both in erythroid cultures and in a transgenic mouse model. *Blood Cell. Mol. Dis.* **2010**, 44, 100–106.
3. Daniela, C.; Alessandro, C.; Giuseppina, L.; Nicola, C.; Maurizio, C.; Gaia, D.G.; Mara, R.; Fabrizio, V.; Cesare, F.; Carlo, M.C. Anthracycline-induced cardiomyopathy: clinical relevance and response to pharmacologic therapy. *J. Am. Coll. Cardiol.* **2010**, 55, 213–220.
4. Christopher, M.O.; Walter, J.K.; Douglas, L.M. Highlights of the 2009 scientific sessions of the Heart Failure Society of America. *J. Card. Fail.* **2010**, 16, 2–8.
5. Benjamin, W.E. Identification of anthracycline cardiotoxicity: Left ventricular ejection fraction is not enough. *J. Am. Soc. Echocardiog.* **2008**, 21, 1290–1292.
6. Corradi, F.; Paolini, L.; De Caterina, R. Ranolazine in the prevention of anthracycline-related cardiotoxicity. *GItal Cardiol.* **2013**, 14(6), 424–437.
7. Adão, R.; de Keulenaer G; Leite-Moreira, A.; Brás-Silva, C. Cardiotoxicity associated with cancer therapy: Pathophysiology and prevention strategies. *Rev Port Cardiol.* **2013**, 32(5), 395–409.
8. Brown, T.R.; Vijarnsorn, C.; Potts, J.; Milner, R.; Sandor, G.G.; Fryer, C. Anthracycline induced cardiac toxicity in pediatric Ewing sarcoma: a longitudinal study. *Pediatr Blood Cancer.* **2013**, 60(5), 842–848.
9. Michael, S.E.; Daniel, D.; Von, H.; Benjamin, R.S. A historical perspective of anthracycline cardiotoxicity. *Heart fail. clin.* **2011**, 3(7), 363–372.
10. Rene, K.; Vojtech, A.; Jan, H.; Tomas, E.; Svatopluk, S.; Jaroslav, V.; Burda, E.; Marie, S. Anthracyclines and ellipticines as DNA-damaging anticancer drugs. *Recent adv. Pharmac. Therap.* **2012**, 1(133), 26–39.
11. Filip, S.E.; Ágnes, B.; Lucas, L.; Tiina, S.; István, Z.; Gyula, S.; János, W.; Reko, L. Cytotoxic activity of some glycoconjugates including saponins and anthracyclines. *Carbo. Res.* **2012**, 15(356), 295–298.
12. Zhao, P.; Xu, L.C.; Huang, J.W.; Fu, B.; Yu, H.C.; Ji, L.N. DNA binding and photocleavage properties of a novel cationic porphyrin-anthraquinone hybrid. *Biophys. Chem.* **2008**, 134, 72–83.
13. Zhao, P.; Xu, L.C.; Huang, J.W.; Fu, B.; Yu, H.C.; Ji, L.N. DNA binding and photocleavage properties of cationic porphyrin-anthraquinone hybrids with different lengths of links. *Bioorg. Chem.* **2008**, 36, 278–287.
14. Zhao, P.; Xu, L.C.; Huang, J.W.; Fu, B.; Yu, H.C.; Ji, L.N. Tricationic pyridium porphyrins appending different peripheral substituents: Experimental and DFT studies on their interactions with DNA. *Biophys. Chem.* **2008**, 135, 102–109.
15. Reichmann, M.E.; Rice, S.A.; Thomas, C.A.; Doty, P. A further examination of the molecular weight and size of desoxypentose nucleic acid. *J. Am. Chem. Soc.* **1954**, 76, 3047–3053.
16. Chaires, J.B.; Leng, F.F., Przewloka, T.; Fokt, I.; Ling, Y.H.; Roman, P.S.; Waldemar, P. Structure-based design of a new bisintercalating anthracycline antibiotic. *J. Med. Chem.* **1997**, 40, 261–266.
17. Portugal, J.; Derek, J.C.; John, O.T.; Neus, F.M.; Teresa, P.; Izabela, F.; Waldemar, P.; Jonathan, B.C. A new bisintercalating anthracycline with picomolar DNA binding affinity. *J. Med. Chem.* **2005**, 48, 8209–8219.
18. Felix, K.; Ulrich, B.; Peter, S.; Michael, K.; Heike, Z.; Thomas, R.; Heinz, H.F.; Clemens, U. Synthesis of new maleimide derivatives of daunorubicin and biological activity of acid labile transferrin conjugates. *Bioorg. Med. Chem. Lett.* **1997**, 7, 617–622.
19. Pasternack, R.F.; Gibbs, E.J.; Villafrancas, J.J. Interactions of porphyrins with nucleic acids; *Biochem.* **1983**, 22, 2406–2414.
20. Masaaki, T.; Ashish, K.S.; Elvis, N. Enhanced conformational changes in DNA in the presence of mercury(II); cadmium(II) and lead(II) porphyrins. *J. Inorg. Biochem.* **2003**, 94, 50–58.
21. Kelly, J.M.; Tossi, A.B.; McConell, D.J.; OhUigin, C. A study of the interactions of some polypyridylruthenium(II) complexes with DNA using fluorescence spectroscopy; topoisomerisation and thermal denaturation. *Nucl. Acids Res.* **1985**, 13, 6017–6034.
22. Sari, M.A.; Battioni, J.P.; Dupre, D.; Mansuy, D.; Lepecq, J.B. Interaction of cationic porphyrins with DNA: importance of the number and position of the charges and minimum structural requirements for intercalation. *Biochem.* **1990**, 29, 4205–4215.
23. Fang, Y.Y.; Ray, B.D.; Caussen, C.A.; Lipkowitz, K.B.; Long, E.C. Ni(II)·Arg-Gly-His−DNA Interactions: Investigation into the Basis for Minor-Groove Binding and Recognition, *J. Am. Chem. Soc.* **2004**, 126, 5403–5412.

24. Han, M.J; Gao, L.H.; Lu, Y.Y.; Wang, K.Z. Ruthenium(II) Complex of Hbopip: Synthesis; Characterization; pH-Induced Luminescence "Off−On−Off" Switch; and Avid Binding to DNA. *J. Phys. Chem. B* **2006**, 110, 2364–2371.
25. Zhu, L.Z.; Cao, X.H.; Chen, W.L.; Zhang, G.H.; Sun, D.X.; Wang, P.G. Syntheses and biological activities of daunorubicin analogs with uncommon sugars. *Bioorg. Med. Chem.* **2005**, 13, 6381–6387
26. David, T.B.; Joseph, E.C.; Jaimie, R.A.; Lori, M.I.; Kan, Y.Z; Williams, L.D.; Bottomley, L.A.; Schuster, G.B. Anthraquinone photonuclease structure determines its mode of binding to DNA and the cleavage chemistry observed. *J. Am. Chem. Soc.* **1997**, 119, 5043–5044.
27. Rosma1en, A.V.; Cu11inane, C.; Cutts, S.M. Stabi1ity of adriamycin- induced DNA adducts and interstrand cross links. *Nucleic Acid. Res.* **1995**, 23 (1), 42–47.
28. Fiel, R.J.; Howard, J.C.; Mark, E.H.; Gupta, N.D. Interaction of DNA with a porphyrin ligand evidence for intercalation. *Nucleic Acids Res.* **1979**, 6, 3093–3118.
29. Satyanarayana, S.; Dabrowiak, J.C.; Chaires, J.B. Neither. DELTA. - nor .LAMBDA.-tris(phenanthroline)ruthenium(II) binds to DNA by classical intercalation; *Biochem.* **1992**, 31, 9319–9324.
30. Satyanaryana, S.; Daborusak, J.C.; Chaires, J.B. Tris(phenanthroline)ruthenium(II) enantiomer interactions with DNA: Mode and specificity of binding. *Biochem.* **1993**, 32, 2573–2584.
31. Maáirá00B4;ın E.A.; Barrett, G.M.; Brian, M.H. Binding of octa-plus porphyrazines to DNA. *J. Inorg. Biochem.* **2000**, 80, 257–260.
32. Kang, J.W.; Wu, H.X.; Lu, X.Q.; Wang, Y.S.; Zhou, L. Study on the interaction of new water-soluble porphyrin with DNA. *Spectrochim Acta; Part A* **2005**, 61, 2041–2047.
33. Ren, J.S.; Chaires, J.B. Sequence and structural selectivity of nucleic acid binding ligands. *Biochem.* **1999**, 38, 16067–16075.
34. Mettath, S.; Munson, B.R.; Pandey, R.K. DNA interaction and photocleavage properties of porphyrins containing cationic substituents at the peripheral position. *Bioconjugate Chem.* **1999**, 10, 94–102.
35. Mehta, G.; Muthusamy, S.; Maiya, B.G.; Arounaguiri, S. Porphyrin-anthraquinone hybrids: Wavelength dependent DNA photonucleases. *Tetrahedron Lett.* **1997**, 38, 7125–7128.
36. Zhao, P.; Huang, J.W.; Ji, L.N. Metal complexes of porphyrin-anthraquinone hybrids: DNA binding and photocleavage specificities. *J. Coord. Chem.* **2011**, 64, 1977–1990.
37. James, R.D.; Petter, D., Anthony, H., George, P., Marie-Claude, R. Metal phthalocyanines and porphyrins as photosensitizers for reduction of water to hydrogen. *Coord. Chem. Rev.* **1982**, 44, 83–126.
38. Ishikawa, Y.; Yamakawa, N.; Uno, T. Potent DNA photocleavage by zinc(II) complexes of cationic bis-porphyrins linked with aliphatic diamine. *Bioorg. Med. Chem.* **2002**, 10, 1953–1957.
39. Ishikawa, Y.; Yamakawa, N.; Uno, T. Efficient photocleavage of DNA by cationic porphyrin–acridine hybrids with the effective length of diamino alkyl linkage. *Chem. Pharm. Bull.* **2001**, 49, 1531.
40. Armitage, B. Photocleavage of Nucleic Acids. *Chem. Rev.* **1998**, 98, 1171–1200.